American Journal of Engineering Research (AJER)
e-ISSN: 2320-0847 p-ISSN : 2320-0936
Volume-8, Issue-6, pp-59-70
www.ajer.org
Research Paper Open Access

Mixed Convection Heat Transfer of Nanofluid in a Lid-Driven Porous Medium Square Enclosure with Pairs of Heat Source-Sinks

M. Jahirul Haque Munshi[1*], Nusrat Jahan[2], Golam Mostafa[1]
[1*]*Department of Mathematics, Hamdard University Bangladesh (HUB), Hamdard Nagar, Gazaria, Munshigonj-1510, Bangladesh*
[2]*Department of Science and Humanities, Bangladesh Army International University of Science and Technology (BAIUST), Cumilla Cantonment, Bangladesh*
[*]*Corresponding author: M. Jahirul Haque Munshi (jahir.buet.bd@gmail.com)*

ABSTRACT: *Mixed convection heat transfer of nanofluid in a lid-driven porous medium square enclosure with several pairs of heat source-sinks has been numerically simulated in this paper. The $Cu - H_2O$ nanofluid is tested and working fluid as $Pr = 6.2$. Two-dimensional Navier-Stokes and energy equations are solved using the finite element method (FEM). Effects on non-dimentional parameters such as Darcy number, Grashof number, Reynolds number, and nanometer size less than 100 and type (Cu) on the heat transfer rate and distribution of nanoparticles are investigated. The simulation results indicate that the nanoparticles for each Darcy number, Grashof number and Reynolds number at which the maximum heat transfer rate occurs. The presented results are validated by favourable comparisons with previously published result. The results of the problem are presented in graphical and tabular forms and discussed. Also results are presented in the form of streamlines, isotherms contours, velocity and dimensional temperature as well as Nusselt number and average Nusselt number along the several pairs of heat source-sinks considered. Moreover, $Cu - H_2O$ nanofluid has greater merit to be used for the heat transfer enhancement.*
KEYWORDS: *Mixed convection, Square cavity, Porous medium, FEM and Source-sinks.*

Date of Submission: 05-05-2019 Date of acceptance: 07-06-2019

NOMENCLATURE

Gr Grashof number	Greek symbols
g gravitational acceleration	**α** thermal diffusivity
L length of the cavity	**β** Volumetric coefficient of thermal expansion
Nu Nusselt number	**ν** kinematic viscosity of the fluid
P dimensional pressure	**θ** non-dimensional temperature
Pr Prandtl number	**ρ** density of the fluid
p pressure	**ψ** non-dimensional stream function
Ra Rayleigh number	
Re Reynolds number	Subscripts
Ri Richardson number	**c** cold wall
T dimensional temperature	**h** hot wall
U, V non-dimensional velocity components	
u, v velocity components	
X, Y non-dimensional Cartesian coordinates	
x, y Cartesian coordinates	

I. INTRODUCTION

Nanofluid technology has emerged as a new enhanced heat transfer technique in recent years. Nanofluid is made by adding nanoparticles and a surfactant into a base fluid can greatly enhance thermal conductivity and convective heat transfer. The diameters of nanoparticles are usually less than 100 nm which improves their suspension properties. Darcy's law is a phenomenological derived constitutive equation that describes the flow of a fluid through a porous medium. The Buoyancy-induced convection happens in a great number of industrical applications such as indoor ventilation with radiators, cooling electrical components,

cooling reactors and heat exchangers. In the recent past, a number of studies have been conducted to investigate the flow and heat transfer characteristics in lid-driven porous medium square cavities. Only the relevant ones are cited in this paper.

Researchers have studied the concept from various perspectives. For examples, Khanafer and Aithal [1] were concentrated on the effect of mixed convection and heat transfer characteristics in a lid-driven cavity with a circular body inside. The results showed that the average Nusselt number increases with an increase in the radius of the cylinder for various Richardson numbers and the optimal heat transfer results are obtained when placing the cylinder near the bottom wall. Islam et al [2] performed a numerical simulation on a lid-driven cavity with an isothermally heated square blockage. Their results showed that Richardson number, size and location of the heater eccentricities affect the average Nusselt number of heater. Kalteh et al [3] investigated laminar mixed convection of nanofluid in a lid-driven square cavity with a triangular heat source and found that increasing the nanoparticle diameter leads to decreases in the heat transfer rate at any Ri. Talebi et al. [4] studied mixed convection of nanofluids inside the differentially heated cavity (DHC). They showed that heat transfer rate has a direct relationship with Rayleigh number and nanoparticle concentration. They also showed that at a given Reynolds number the stream function increases with increasing volume fraction of nanoparticles, in particular at the higher Rayleigh number. Muthtamilselvan and Doh [5] investigated steady state two-dimensional mixed convection in a lid-driven square cavity filled with Cu-water nanofluid. They found that Richardson number and solid volume fraction affect the fluid and heat transfer in the cavity. Boulahia and Sehaqui [6] analyzed a natural convection of nanofluid in a square cavity including a square heater. They found that by increasing size of the heater, the heat transfer rate enhances. Boulahia et al. [7] investigation the mixed convection heat transfer of nanofluid in a lid driven square cavity with three triangular heating blocks and they found by decreasing the Richardson number and increasing the volume fraction of nanoparticles the rate of convective heat transfer is increased. Work of Oztop et al. [8] can be mentioned as example of such studies, in which they numerically studied mixed convection in square cavities with two moving walls. Their results suggest that when the vertical walls move upwards in the same direction, the heat transfer decreases significantly compared to when the vertical walls move in opposite directions. Parvin et al. [9] investigated the effect of Prandtl unmber on forced convection in a two sided open enclosure using Nanofluid. They found maximum rate of heat transfer is obtained for the higher Pr and lowest A and the mean temperature of the fluid in the channel decrease with rising Pr and diminishing A. Nasrin et al. [10] considered different physical parameters on forced convection along a horizontal corrugated pipe with Nanofluid. Their results showed that the structure of the fluid flow and temperature field through the pipe is found to be significantly dependent upon the mentioned parameters. Rahman et al. [11] has investigated numerically unsteady natural convection in Al_2O_3-Water nanofluid filled in isosceles triangular enclosure with sinusoidal thermal boundary condition on bottom wall. Mansour et al. [12] has observed that the numerical simulation of mixed convection flows in a square lid-driven cavity partially heated from below using nanofluid. Ahmed et al. [13] solve mixed convection from a discrete heat source in enclosures with two adjacent moving walls and filled with micropolar nanofluids. Malvandi et al. [14] investigated slip flow of alumina/water nanofluid in a circular microchannel. They found that nanoparticles move from the hot wall towards the core region where fluid temperature is lower than elsewhere and result in a non-uniform nanoparticle distribution. In a similar work, Garoosi et al. [15] performed two phase simulation of natural convection and mixed convection of the nanofluid in a square cavity. Munshi et al. [16] investigated numerically effect of hydromagnetic mixed convection double lid-driven square cavity with inside elliptic heated block.

On the basis of the above literature review, it appears that very little work reported on the lid driven porous square enclosure. There is no present study on mixed convection heat transfer of nanofluid in a lid-driven porous medium square cavity with pairs of heat source-sinks. The key parameters in this study are the nanoparticles volume fraction $\varphi = 5\%$, nanoparticle type Cu, Darcy number$(1e^{-5} \leq Da \leq 1e^{-2})$, Grashof number$(10^3 \leq Gr \leq 10^6)$, Reynolds number$(1 \leq Re \leq 100)$. The objective of the present study to analyze the increase of the heat transfer rate in fluid through porous cavity, also increase of the lid-driven constant velocity to high light the applicability of the approach.

II. PHYSICAL MODEL

The physical models under consideration numerical simulation of hydrodynamics mixed convection heat transfer of a nanofluid in a lid-driven porous square cavity with several pairs of heat sources and sinks. The cavity is a square with the height of L. The cavity is filled with Cu-H_2O and the thermophysical properties of Cu nanoparticles and water (Pr = 6.2) as base fluid are listed in Table 1. The square cavity is maintained at heated temperature T_h and cold temperature T_c. Other parts of the cavity walls are all thermally insulated. The top lid moves right to left and bottom lid moves left to right. The flow is assumed to be incompressible, two dimensional, steady, are laminar.

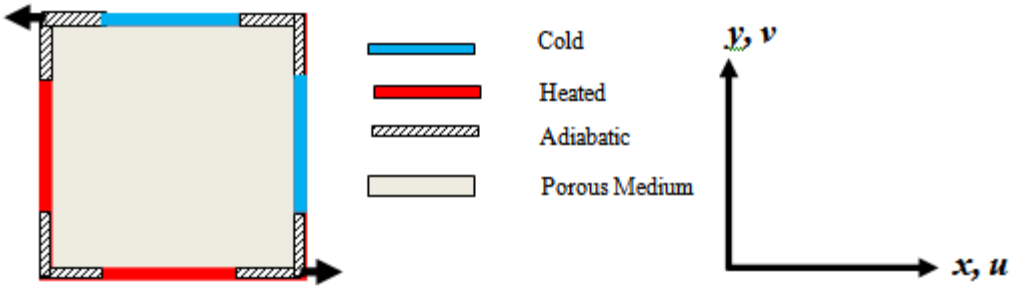

Fig.1. Schematic View of the Cavity with Boundary Conditions Considered in the Present Paper.

III. MATHEMATICAL FORMULATION

The fluid is considered as incompressible, Newtonian and the flow is assumed to be laminar. The governing equations for steady two-dimensional mixed convection flow in the porous cavity using conservation of mass, momentum and energy can be written as:

$$\frac{\partial u}{\partial x}+\frac{\partial v}{\partial x}=0 \tag{1}$$

$$\rho_{nf}\left(u\frac{\partial u}{\partial x}+v\frac{\partial u}{\partial y}\right)=-\frac{\partial p}{\partial x}+\mu_{nf}\nabla^2 u-\frac{(\rho\beta)_{nf}}{k}\nu u \tag{2}$$

$$\rho_{nf}\left(u\frac{\partial v}{\partial x}+v\frac{\partial v}{\partial y}\right)=-\frac{\partial p}{\partial y}+\mu_{nf}\nabla^2 v-\frac{(\rho\beta)_{nf}}{k}\nu v+(\rho\beta)_{nf}g\beta(T-T_c) \tag{3}$$

$$u\frac{\partial T}{\partial x}+v\frac{\partial T}{\partial y}=\alpha_{nf}\nabla^2 T \tag{4}$$

where x, y are the distance measured along the horizontal and vertical directions, u, v are the velocity components in the x and y directions, ρ is the density, p is the pressure, ν is the kinematic viscosity, k is the permeability of the porous medium, g is the acceleration due to gravity, α is the thermal diffusivity, β is the volume expansion coefficient, T is the temperature.

Also, the effective density of the nanofluid is described by the following equation

$$\rho_{nf}=(1-\phi)\rho_f+\phi\rho_s \tag{5}$$

where ϕ denotes the solid volume fraction of nanofluid. The thermal diffusivity of the nanofluid can be stated by the following equation

$$\alpha_{nf}=\frac{k_{nf}}{(\rho c_p)_{nf}} \tag{6}$$

where heat capacitance of nanofluids is designated by $(\rho c_p)_{nf}$ and can be found by

$$(\rho c_p)_{nf}=(1-\phi)(\rho c_p)_f+\phi(\rho c_p)_s \tag{7}$$

Furthermore, the thermal expansion coefficient of the nanofluid is $(\rho\beta)_{nf}$ where

$$(\rho\beta)_{nf}=(1-\phi)(\rho\beta)_f+\phi(\rho\beta)_s \tag{8}$$

Moreover, μ_{nf} is the dynamic viscosity of the nanofluid and can be obtained by

$$\mu_{nf}=\frac{\mu_f}{(1-\phi)^{2.5}} \tag{9}$$

Ahmed et al. [13] described the effective thermal conductivity of nanofluid as follows:

$$k_{nf}=\frac{k_s+2k_f-2\phi(k_f-k_s)}{k_s+2k_f+\phi(k_f-k_s)}\times k_f \tag{10}$$

Where thermal conductivity of the nanoparticle is the k_s and thermal conductivity of base fluid is the k_f.

IV. THERMOPHYSICAL PROPERTIES

Table 1: Thermo-physical properties of water and nanoparticles [13]:

Physical properties	H_2O	CuO
C_p (J/Kg K)	4179	385
ρ (Kg/m^3)	997.1	8933
K (W/mK)	0.613	401
β (K^{-1})	21×10^{-5}	1.67×10^{-5}
$\mu(kg\ m^{-1}\ s^{-1})$	0.855×10^{-3}	-

4.1 Boundary Conditions

The boundary conditions for the present problem are specified as follows:

On the top wall: $u=-U_0,\ v=0,\ T=T_c,\ for\ (1-\varepsilon)/2 \le X \le (1+\varepsilon)/2$

$$u=-U_0,\ v=0,\ \frac{\partial T}{\partial y}=\begin{cases}0,\ for\ 0<X<(1-\varepsilon)/2\\ 0,\ for\ (1+\varepsilon)/2<X<1\end{cases}$$

On the right wall: $u=0\ v=0,\ T=T_c,\ for\ (1-\varepsilon)/2 \le Y \le (1+\varepsilon)/2$

$$u=0,\ v=0,\ \frac{\partial T}{\partial x}=\begin{cases}0,\ for\ 0<Y<(1-\varepsilon)/2\\ 0,\ for\ (1+\varepsilon)/2<Y<1\end{cases}$$

On the bottom wall: $u=U_0,\ v=0,\ T=T_h,\ for\ (1-\varepsilon)/2 \le X \le (1+\varepsilon)/2$

$$u=U_0,\ v=0,\ \frac{\partial T}{\partial y}=\begin{cases}0,\ for\ 0<X<(1-\varepsilon)/2\\ 0,\ for\ (1+\varepsilon)/2<X<1\end{cases}$$

On the left wall: $u=0\ v=0,\ T=T_h,\ for\ (1-\varepsilon)/2 \le Y \le (1+\varepsilon)/2$

$$u=0,\ v=0,\ \frac{\partial T}{\partial x}=\begin{cases}0,\ for\ 0<Y<(1-\varepsilon)/2\\ 0,\ for\ (1+\varepsilon)/2<Y<1\end{cases}$$

Using the following dimentionless parameters, the governing equations can be converted to the dimentionless form:

$$X=\frac{x}{L},Y=\frac{y}{L},U=\frac{u}{U_0\alpha_f},V=\frac{v}{U_0\alpha_f},P=\frac{p}{\rho_{nf}U_0^2},\theta=\frac{T-T_c}{T_h-T_c},P_r=\frac{\upsilon_f}{\alpha_f},Da=\frac{K}{L^2},$$
$$Re=\frac{U_0L}{\upsilon_f},Gr=\frac{g\beta(T_h-T_c)L^3}{{\upsilon_f}^2}$$

Note that, thermal diffusivity (α) and kinematic viscosity (ν) in Eq. (4) are defined based on local thermal equilibrium between solid and fluid within a porous control volume Nield et al. [18] where $\alpha=\frac{k_{eff}}{\phi\rho_0C_{pf}}$ and $\nu=\frac{\mu_f}{\rho_0}$. Here k_{eff} is the effective thermal conductivity of the porous matrix, ϕ is the porosity, C_{pf} is the specific heat of fluid, μ_f is the viscosity of fluid and $\rho_0=\rho$ is the density of fluid at $\theta=0$.

4.2 Dimensional Analysis

The governing equations for steady two-dimensional mixed convection flow in a lid-driven porous square cavity using conservation of mass, momentum and energy can be written with the following dimensionless variables:

$$\frac{\partial U}{\partial X}+\frac{\partial V}{\partial Y}=0 \tag{11}$$

$$U\frac{\partial U}{\partial X}+V\frac{\partial U}{\partial Y}=-\frac{\partial P}{\partial X}+\frac{1}{Re}\frac{\rho_f}{\rho_{nf}}\frac{1}{(1-\varphi)^{2.5}}\nabla^2U-\frac{(\rho\beta)_{nf}}{\rho_{nf}\beta_f}\frac{1}{ReDa}U \tag{12}$$

$$U\frac{\partial V}{\partial X}+V\frac{\partial V}{\partial Y}=-\frac{\partial P}{\partial Y}+\frac{1}{Re}\frac{\rho_f}{\rho_{nf}}\frac{1}{(1-\varphi)^{2.5}}\nabla^2V-\frac{(\rho\beta)_{nf}}{\rho_{nf}\beta_f}\frac{1}{ReDa}V+\frac{(\rho\beta)_{nf}}{\rho_{nf}\beta_f}\frac{Gr}{Re^2}\theta \tag{13}$$

$$U\frac{\partial \theta}{\partial X}+V\frac{\partial \theta}{\partial Y}=\frac{\alpha_{nf}}{\alpha_f}\frac{1}{RePr}\nabla^2\theta \tag{14}$$

The dimensionless boundary conditions for solving the governing equations (11)- (14) are:

On the top wall: $U=-1,V=0,\theta=0,\ for\ (1-\varepsilon)/2 \le X \le (1+\varepsilon)/2$

$$U=-1,V=0,\ \frac{\partial \theta}{\partial y}=\begin{cases}0,\ for\ 0<X<(1-\varepsilon)/2\\ 0,\ for\ (1+\varepsilon)/2<X<1\end{cases}$$

On the right wall: $U=0,V=0,\theta=0,\ for\ (1-\varepsilon)/2 \le Y \le (1+\varepsilon)/2$

$$U=0,V=0,\ \frac{\partial \theta}{\partial x}=\begin{cases}0,\ for\ 0<Y<(1-\varepsilon)/2\\ 0,\ for\ (1+\varepsilon)/2<Y<1\end{cases}$$

On the bottom wall: $U=1,V=0,\theta=1,\ for\ (1-\varepsilon)/2 \le X \le (1+\varepsilon)/2$

$$U=1, V=0, \frac{\partial\theta}{\partial y}=\begin{cases}0, & for\ 0<X<(1-\varepsilon)/2\\ 0, & for\ (1+\varepsilon)/2<X<1\end{cases}$$

On the left wall: $U=0, V=0, \theta=1, \quad for\ (1-\varepsilon)/2\le Y\le(1+\varepsilon)/2$

$$U=0, V=0, \frac{\partial\theta}{\partial x}=\begin{cases}0, & for\ 0<Y<(1-\varepsilon)/2\\ 0, & for\ (1+\varepsilon)/2<Y<1\end{cases}$$

For computation of the rate of heat transfer, Nusselt number along the horizontal wall of the enclosure

$$\mathrm{Nu_L}=-\frac{\mathrm{K_{eff}}}{\mathrm{K_f}}\frac{\partial\theta}{\partial X}\Big|_{X=0}$$

Average Nusselt number along the right wall of the cavity is considered to evaluate the overall heat transfer rate and is defined as: $\mathrm{Nu_{ave}}=\int_0^1 \mathrm{Nu_L}\,dY$. The stream function is calculated using $U=\frac{\partial\Psi}{\partial Y}$ and $V=-\frac{\partial\Psi}{\partial X}$.

V. NUMERICAL TECHNIQUE

The nonlinear governing partial differential equations, i.e., mass, momentum and energy equations are transferred into a system of integral equations by using the Galerkin weighted residual finite-element method. The nonlinear algebraic equations so obtained are modified by imposition of boundary conditions. These modified nonlinear equations are transferred into linear algebraic equations with the aid of Newton's method. Lastly, Triangular factorization method is applied for solving those linear equations. For numerical computation and post processing, the software COMSOL Multiphysics is used.

5.1. Code Validation

The computational procedure was validated against various numerical results available in the literature, four different heat convection problems are chosen. The first case is the numerical results of Iwatsu et al (1993) and Oztop et al. (2009) for a top heated moving lid bottom cooled square cavity filled with air Pr = 0.71. Table 7.2 demonstrates an excellent comparison of the average Nusselt number between the present results and the numerical results found in the above literature.

Table 2: Comparison of Average Nusselt number at the top wall between the present results and those reported in the literature

Ri	Average Nusselt number at the top wall		
	Iwatsu et al (1993)	Oztop et al. (2009)	Present
1	1.34	1.30	1.40
0.1	3.62	3.63	3.79
0.01	6.29	6.34	6.31

5.2. Grid Refinement Check

Geometry studied in this article is a mixed convection heat transfer of nanofluid flow in a lid-driven porous square cavity; therefore, several nonuniform grids distribution are considered in this geometry to test and assess grid independence of the present solution scheme. Many numerical runs are performed for evaluating the average Nusselt number and average fluid temperature, as shown in Figure 2. Five different nonuniform grids with the following number of nodes are considered for grid refinement tests: 31,699, 38,787, 48,324, 49,685 and 62, 521. The magnitude of the average Nusselt number and average fluid temperature for 48,324 nodes illustrates a very slight difference with the results obtained for other finer nodes. Hence, the grid of 48,324 nodes has been chosen throughout the simulation to optimize the relation between the accuracy required and the computing time.

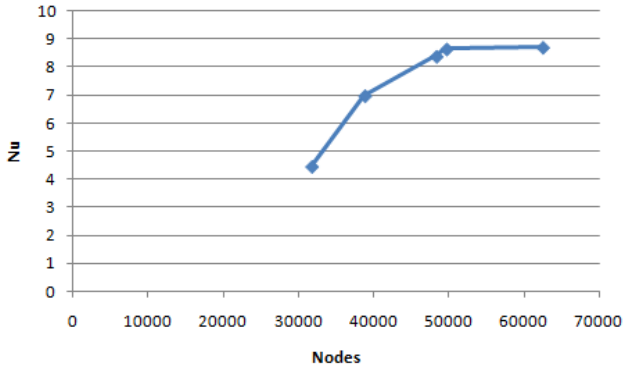

Fig. 2: Grid independency study for Pr = 6.2, Da = 10^{-5}, Re = 10^{2}, Gr = 10^{5} and $\varphi = 5\%$.

5.3. Mess Generation

In finite element method, the mesh generation is the technique to subdivide a domain into a set of sub-domains, called finite elements. The discrete locations are defined by the numerical grid, at which the variables are to be calculated.

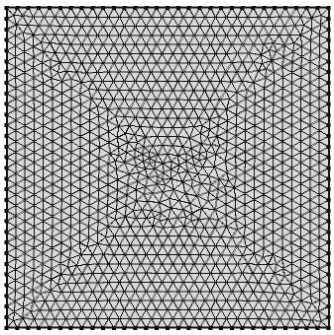

Fig. 3: Mess generation of the lid-driven porous medium square cavity.

The computational domains with irregular geometries by a collection of finite elements make the method a valuable practical tool for the solution of boundary value problems arising the various fields of engineering. Fig. 3 displays the finite element mesh of the present physical domain.

VI. RESULTS AND DISCUSSION:

Mixed convection heat transfer of nanofluid in a lid-driven porous square cavity is simulated. The key parameters in this study are the nanoparticles volume fraction $\varphi = 5\%$, nanoparticle type Cu, Darcy number$(1e^{-5} \leq Da \leq 1e^{-2})$, Grashof number $(10^3 \leq Gr \leq 10^6)$, Reynolds number$(1 \leq Re \leq 100)$.

6.1. Effect of Darcy number on mixed convection

In this section the effects of external and internal heating, nanoparticle volume fraction $\varphi = 5\%$, nanoparticle type Copper and Darcy number $(1e^{-5} \leq Da \leq 1e^{-2})$ on the fluid flow, the heat transfer rate and distribution of the nanoparticles are presented for the mixed convection configuration, Figure 4 shows streamlines and isotherms at different Darcy number.

Figure 4 illustrate the streamlines and isotherms inside the cavity with the effect of Darcy numbers. As seen from the Figure, a pair of counter rotating vortex is formed left and right wall of the cavity. Also seen form the Figure, isotherms line bending the left and right wall of the cavity when Darcy increasing isotherms condense left and right wall which means increasing heat transfer through convection.

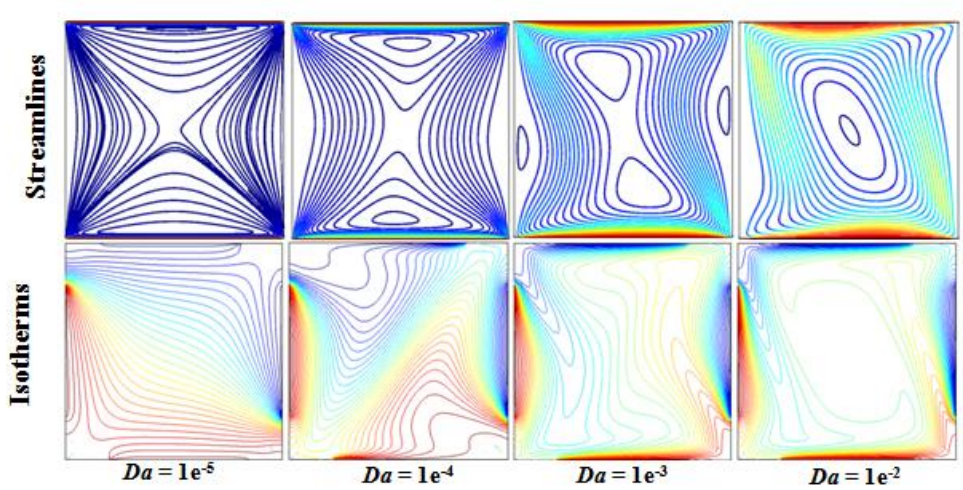

Fig. 4. Streamlines and Isotherms for different values of Darcy numbers Da = $1e^{-5}$, $1e^{-4}$, $1e^{-3}$, $1e^{-2}$ when Re = 100, Gr = 10^4.

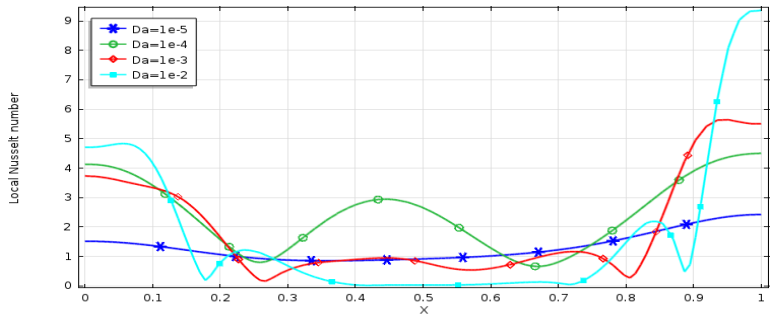

(a)

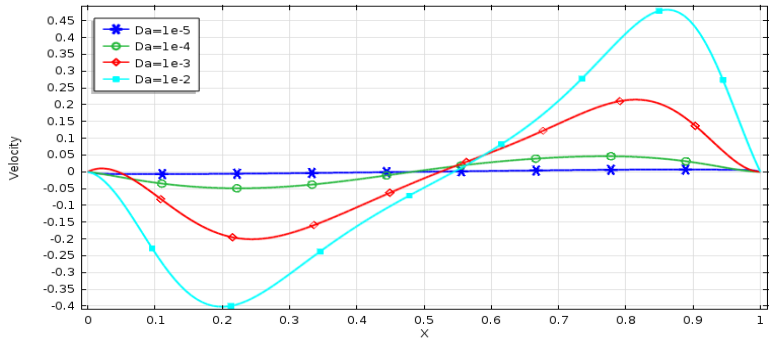

(b)

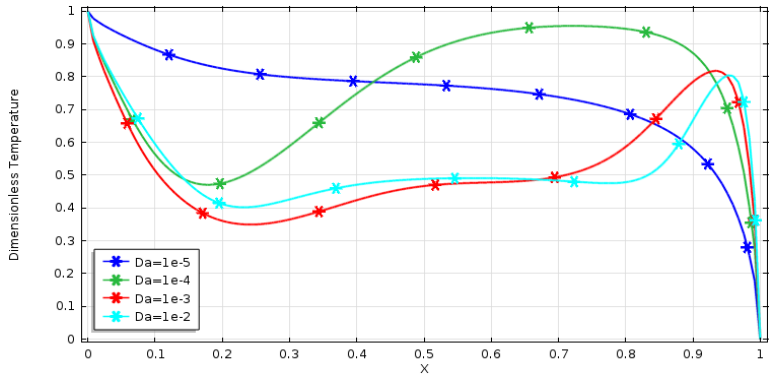

(c)

Fig. 5. Variation of (a) Local Nusselt number (b) Vertical velocity profiles and (c) Vertical dimensionless temperature profiles along horizontal wall while Gr = 10^5, Re = 100 and Pr = 6.2

Variation of the local Nusselt number along the bottom wall with the Darcy numbers are shown in Figure 5(a). As seen from the Figure in whole portion of the cavity the local Nusselt number increase with increasing in the Darcy number. Variation of vertical velocity profile for different values of Darcy numbers along horizontal wall are shown in Figure 5(b). Owing to the symmetry in thermal boundary conditions, the velocity is symmetrical with respect to the vertical midline of the cavity. When the Darcy number increase the velocity profiles has larger change. Figure 5(c) presents the temperature profiles along the bottom wall for different values of Darcy numbers. As seen from the Figure, temperature value is decrease with increasing of Darcy numbers. For lower values of Darcy number temperature value has larger change but higher Darcy number temperature value has smaller change.

6.2 Effect of Grashof number on mixed convection

Figure 6 illustrates the streamlines and isotherms in various Grashof numbers. We can see from the streamlines of Figure 6 that more fluid raised inside the cavity. As seen from the Figure *Gr* increasrs vortex cells created on the middle side of the cavity. Conduction dominant heat tranafer is obseorved from the isotherms in Figure 6. It can be seen from the Figure that the isotherms appear parallel to the heated walls for the left and right walls and isotherms lines are more bending middle of the square cavity.

From the isotherms it is observed that with increase in Grashof number and two square heating blocks and two cold blocks is considered for heat transfer analysis, mixed convection is suppressed and heat transfer occurs mainly through convection. With increase in Grashof number, isotherms are concentrates near the left wall to right wall of middle positions, which means increasing heat transfer through convection.

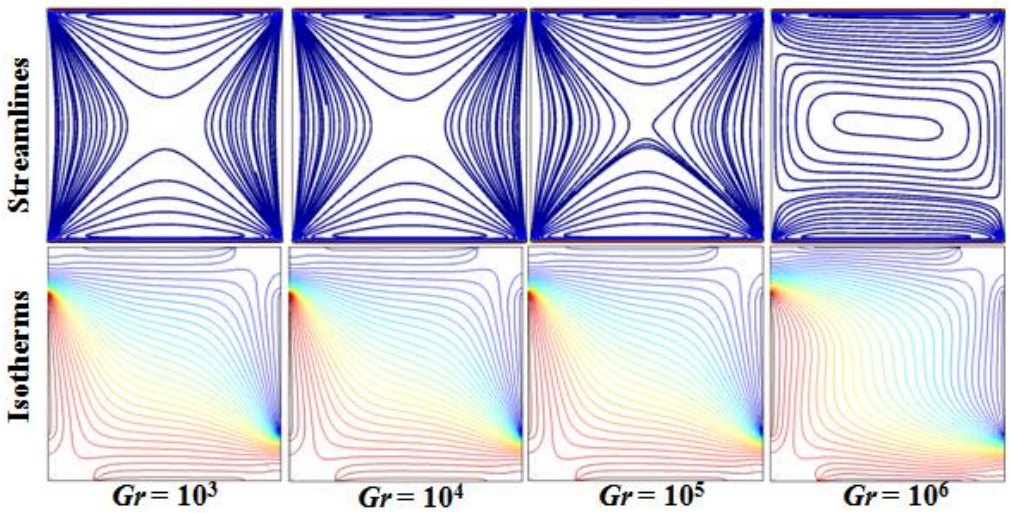

Fig. 6. Streamlines and Isotherms for different values of Grashof numbers $Gr = 10^3$-10^6 when $Re = 100$, $Da = 10^{-5}$.

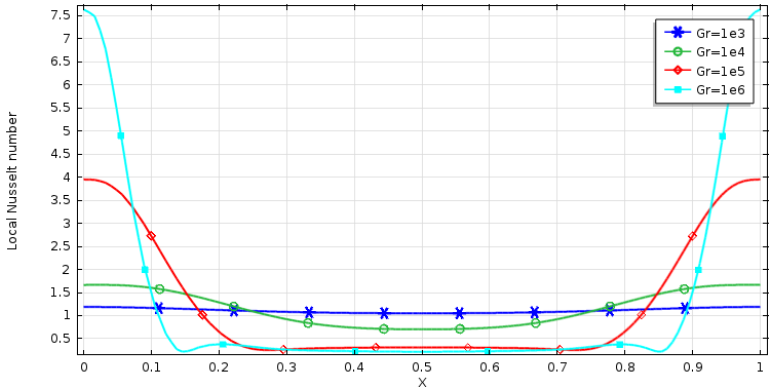

(a)

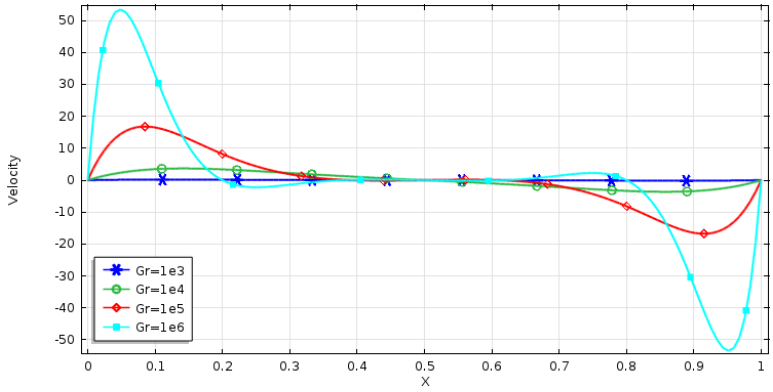

(b)

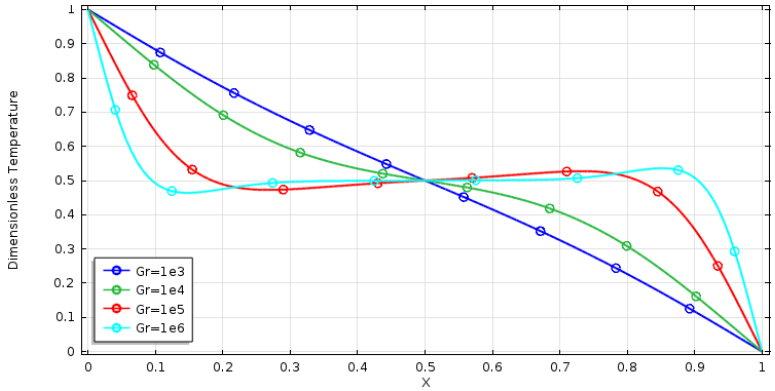

(c)

Fig.7 . Effect on different values of Reynolds numbers on (a) Local Nusselt number (b) Velocity profiles and (c) Dimensionless temperature while Gr = 10^5, Re = 100 and Pr = 6.2

6.3 Effect of Reynolds number on mixed convection

Mixed convection heat transfer of the nanofluid is simulated in the square cavity. The key parameters in this study are external and internal heating, nanoparticles volume fraction $\varphi = 0.05$, nanoparticle type Cu, Reynolds number $(1 \leq \mathrm{Re} \leq 10^2)$ when $\mathrm{Gr} = 10^5$, $\mathrm{Da} = 1e^{-5}$. Figure 8 shows streamlines and isotherms at different Reynolds numbers. The streamlines and isotherms of Cu-water nanofluids are also shown. It can be seen from Figure 8 circulation vortex is formed inside the cavity and isotherms are uniformly distributed, which indicates that conduction is the main heat transfer mechanism. By increasing the Re, the intensity of the flow and convection inside the cavity increases, and as a result other small vortex start to from the cavity. In general, isotherms become more distorted by increasing the Re due to the stronger convection effects.

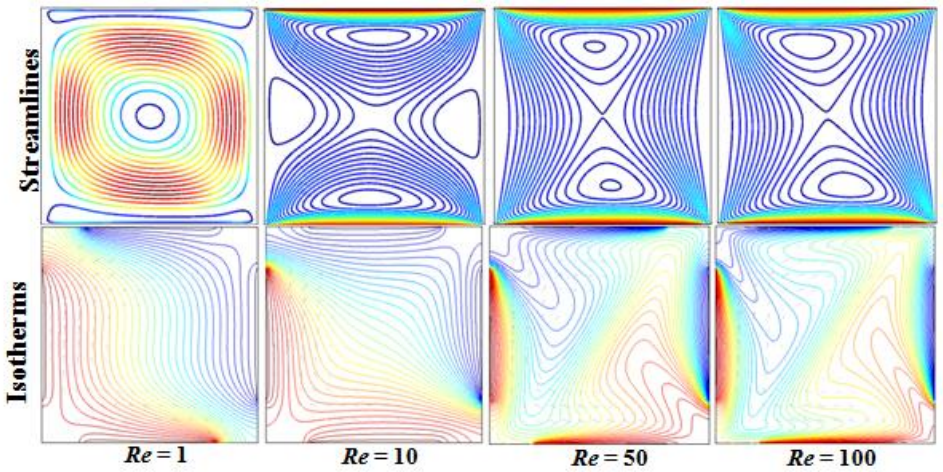

Fig. 8. Streamlines and Isotherms for different values of Reynolds numbers Re = 1-10^2 when Gr = 10^4, Da = 10^{-5}.

Variation of the local Nusselt number along the bottom wall of the cavity with different Reynolds number when Gr = 10^5, Re = 100 and Pr = 6.2 are shown in Figure 9. As seen from the Figure in the whole portion minimum and maximum shape curve of the local Nusselt number line increases with increase in the Reynolds number.

Variation of the vertical velocity components along the bottom wall for different values of Reynolds numbers are shown in Figure 9. As seen from the Figure lower value of Reynolds number value of velocity has linearly change but for the higher value of Reynolds number value of velocity has more significance change.

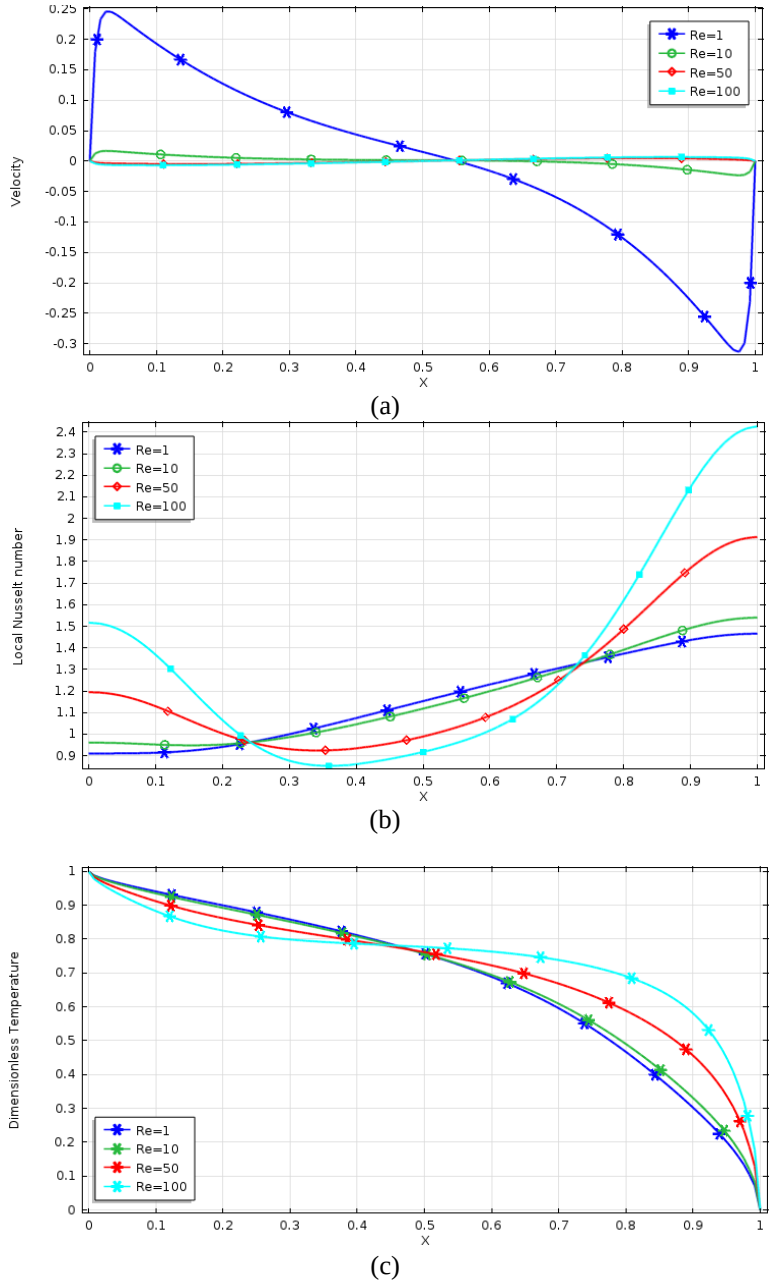

Fig. 9. Effect on different values of Reynolds numbers on (a) Local Nusselt number (b) Velocity and (c) Dimensionless temperature while Gr = 10^5, Re = 100 and Pr = 6.2

In Figure 9 present the dimentionless temperature profiles along the bottom wall for different Reynolds numbers. As seen from the Figure, maximum and minimum shape curves inside the cavity. When X < 0.5 temperature value has maximum and X > 0.5 temperature value has minimum.

Variation of average Nusselt number versus Darcy number different values of Grashof number are shown in Figure 10. Generally average Nusselt number increases with increasing Darcy number. In particular

maximum heat transfer rate is attained for high Darcy number a large size of porous larger has high permeability which permits enormous amount of heat to transfer within the porous medium.

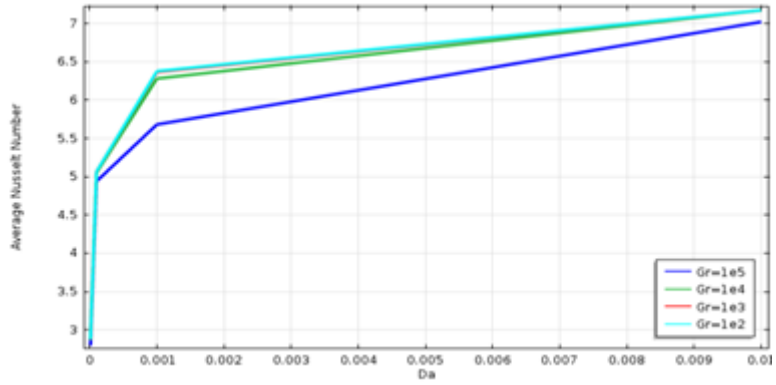

Fig. 10: Variation of average Nusselt number versus Darcy number for different Grashof number along the top wall where Pr = 6.2 and Re = 100.

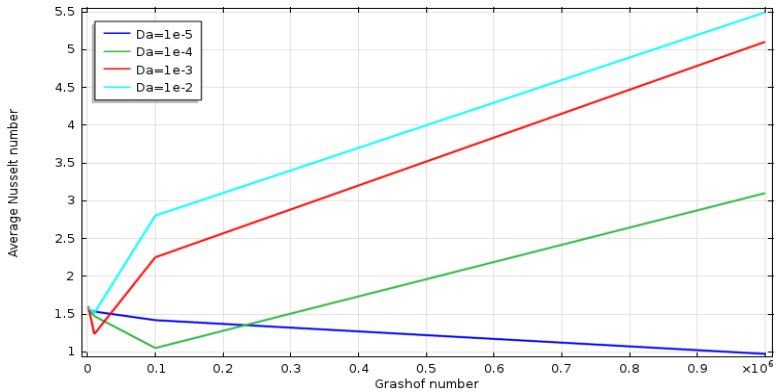

Fig. 11: Variation of average Nusselt number versus Grashof number for different Darcy number along the top wall where Pr = 6.2 and Re = 100.

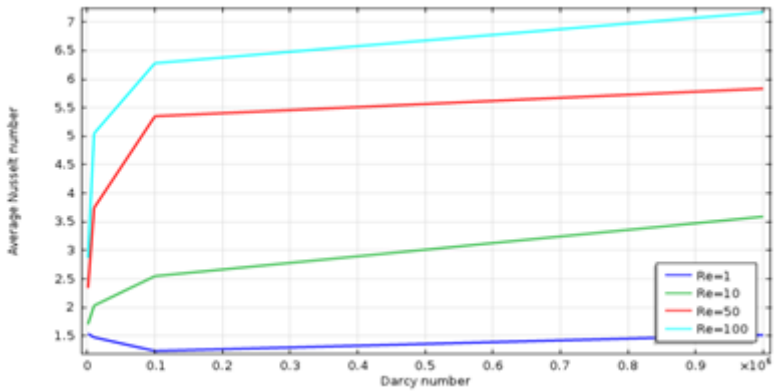

Fig. 12: Variation of average Nusselt number versus Darcy number for different Reynolds number along the top wall where Pr = 6.2 and Gr = 10^5.

The influence of Darcy number on average Nusselt number versus Grashof number for top wall is displayed in Fig. 11 at Pr = 6.2 and Re = 100. It is also evident from this figure that values of average Nusselt number grows as a percentage of Darcy number increases from $1e^{-5}$ to $1e^{-2}$. Variation of average Nusselt number versus Darcy number for different Reynolds number along the top wall is displayed in Fig. 12 at Pr = 6.2 and Gr = 10^5. It is clearly observed that adding Reynolds number inside the porous enclosure cause an increase in the average Nusselt number. Also rate of increment or the heat transfer clearly depends on the value of Reynolds number.

VII. CONCLUSIONS

A computational study of hydrodynamic mixed convection heat transfer of nanofluid in a lid-driven porous medium square cavity with several pairs of heat source-sinks. The results are obtained for a wide range of pertinent dimensionless groups such as Darcy number, Grashof number, and Reynolds number. For all cases considered, two or more counter rotating eddies were formed inside the cavity regardless the Darcy number and the Reynolds numbers. In view of the obtained results, the following findings are précised:

i. The flow characteristics and heat transfer mechanism inside the enclosure are strongly dependent on the Darcy number.
ii. Significant changes occur in the flow and thermal fields for both source and sink whichcause high heat transfer.
iii. As Darcy increases average Nusselt number also increases. In particular, high heattransfer rate is achieved for higher Darcy number.
iv. The velocity of the fluid flow augmented by the increase of Cu nanoparticle which results increase in heat transfer rate.

REFERENCES

[1]. Khanafar, K., Aithal, S. M., "Laminar mixed convection flow and heat transfer characteristics in a lid-driven cavity with a circular cylinder', Int. J. Heat Mass Transf., vol. 66, pp. 200- 209, 2013.
[2]. Islam, A. W., Sharif, M. A. R., Carlson, E. S., "Mixed convection in a lid driven square cavity with an isothermally heated square blockage inside", Int. J. Heat Mass Transf., vol. 55, pp. 5244-5255, 2012.
[3]. Kalteh, M., Javaherdeh, K., Azarbarzin, T., "Numerical solution of nanofluid mixed convection heat transfer in a lid-driven square cavity with a triangular heat source", Powder Technol., vol. 253, pp. 780-788, 2014.
[4]. Talebi, F., Mahmoudi, A. H., Shahi, M., "Numerical study of mixed convection flows in a square lid-driven cavity utilizing nanofluid", Int. Commun. Heat Mass Transf., vol. 37, pp. 79-90, 2010.
[5]. Muthtamilselvan, M., Doh, D. H., "Mixed convection of heat generating nanofluid in a lid-driven cavity with uniform and non-uniform heating of bottom wall", Appl. Math. Model., vol. 38, pp. 3164-3174, 2014.
[6]. Boulahia, Z., Sehaqui, R., "Numerical Simulation of Natural Convection of Nanofluid in a Square Cavity Including a Square Heater", International Journal of Science and Research (IJSR), ijsr.net, vol. 4, Issue 12, pp. 1718-1722, 2015.
[7]. Boulahia, Z., Wakif, A., Sehaqui, R., "Numerical investigation of mixed convection heat transfer of nanofluid in a lid driven square cavity with three triangular heating blocks", International Journal of Computer Applications, Vol. 143, no. 6, pp. 37-45, 2016.
[8]. Oztop, H. F., Dagtekin, I., "Mixed convection in two-sided lid-driven differentially heated square cavity", Int. J. Heat Mass Transfer, vol. 47, pp. 1761- 1769, 2004.
[9]. Parvin, S., Nasrin, R., Alim, M. A., Hossain, N. F., "Effect of Prandtl Number on Forced Convection in a Two Sided Open Enclosure Using Nanofluid", J. Sci. 5(1), 67-75, 2013.
[10]. Nasrin, R., Alim, M. A., "Analysis of Physical parameters on Forced convection along a horizontal corrugated pipe with Nanofluid", Engineering e-Transaction, Vol. 7, No. 1, pp. 14-22, 2012.
[11]. Rahman, M. M., Hakan F. Oztop, Mekhilef, S., Saidur, R., Khaled Al-Salem, "Unsteady natural convection in Al_2O_3-Water nanofluid filled in isosceles triangular enclosure with sinusoidal thermal boundary condition on bottom wall", Superlattices and Microstructures, vol. 67, pp. 181-196, 2014.
[12]. Mansour, M. A., Mohamed, R. A., Abu-Elaziz, M. M., Ahmed, S. E., "Numerical simulation of mixed convection flows in a square lid-driven cavity partially heated from below using nanofluid", International Communications in Heat and Mass Transfer, vol. 37, pp. 1504-1512, 2010.
[13]. Ahmed, S. E., Mansour, M. A., Hussein, A. K., Sivasankaran, S., "Mixed convection from a discrete heat source in enclosures with two adjacent moving walls and filled with micropolar nanofluids", International Journal Engineering Science and Technology, vol. 19, pp. 364-376, 2016.
[14]. Malvandi, A., Ganji, D. D., "Brownian motion and thermophoresis effects on slip flow of alumina/ water nanofluid inside a certain microchannel in the presence of a magnetic field", Int. J. Therm. Sci., vol. 84, pp. 196-206, 2014.
[15]. Garoosi, F., Bagheri, G. H., Rashidi, M. M., "Two phase simulation of natural convection and mixed convection of the nanofluid in a square cavity", Powder Technology, vol. 275, pp. 239-256, 2015.
[16]. Munshi, M. J. H., Alim, M. A., "Effect of Hydromagnetic Mixed Convection Double Lid Driven Square Cavity with Inside Elliptic Heated Block", Journal of Scientific Research, vol. 9(1), pp. 1-11, 2016.
[17]. Reddy, J. N., "An Introduction to Finite Element Analysis", McGraw-Hill. New York, 1993.
[18]. Nield, D. A., Bejan, A., "Convection in Porous Media, third ed., Springer", Berlin, 2006

M. Jahirul Haque Munshi" Mixed Convection Heat Transfer of Nanofluid in a Lid-Driven Porous Medium Square Enclosure with Pairs of Heat Source-Sinks" American Journal of Engineering Research (AJER), vol.8, no.06, 2019, pp.59-70